JOURNAL OF SOLID STATE CHEMISTRY **122,** 130–138 (1996)
ARTICLE NO. 0092

Synthesis, Crystal Structure, and Magnetic Measurement of Two New Diselenites: $M_2(Se_2O_5)_3$ with M = Fe(III), Cr(III)

Anne-Marie Lafront, Jacques Bonvoisin, and Jean-Christian Trombe[1]

Centre d'Elaboration des Matériaux et d'Etudes Structurales, CEMES-CNRS, 29 rue Jeanne Marvig, BP 4347, 31055 Toulouse Cedex, France

Received July 31, 1995; in revised form November 6, 1995; accepted November 8, 1995

Two new diselenite compounds have been synthetized by solid state reaction and their structures have been determined: $Fe_2(Se_2O_5)_3$ (I) and $Cr_2(Se_2O_5)_3$ (II). Both compounds crystallize in the monoclinic system, with the same space group $P2_1/n$ and moreover the unit cell dimensions are similar: a = 11.325(1) Å, b = 11.038(1) Å, and c = 11.563(2) Å, β = 102.56(1)°, $P2_1/n$, Z = 4, and V = 1411.0(8) Å^3 for (I); a = 10.904(1)) Å, b = 11.369(2) Å, and c = 11.673(2) Å, β = 95.11(2)°, $P2_1/n$, Z = 4, and V = 1441.1(6) Å^3 for (II). In both compounds, the structure is built up from isolated octahedra sharing all their oxygen atoms with $Se_2O_5^{2-}$ groups, thus forming a three-dimensional network. Each diselenite group acts as tetramonodentate ligand. Iron octahedra are more distorted than chromium ones. Some differences appear in the thermal behavior studies of these compounds. The chromium compound presents only a one step process instead of two for the iron compound giving an intermediate phase $Fe_2(SeO_3)_3$. Magnetic measurements reveal a weak antiferromagnetic coupling for both compounds with a transition to a long range magnetic ordering at low temperature T = 32 K for (I).

INTRODUCTION

Studies concerning the selenites of transition elements are of particular interest because of (i) the specific chemistry of the Se(IV) element with the presence of lone pair (1–3) and (ii) the specific architecture of some of these compounds which exhibit a low dimensional character (4, 5). The peculiar role of the lone pair of the Se(IV) in the antiferromagnetic coupling exhibited by copper(II) diselnite has been emphasized (1). Various diselenites of transition elements have already been prepared and their structures determined. Bertaud reported the unit cell constants of iron(III) and chromium(III) diselenites (Table 1) but he failed to solve their structure (3). Besides, the crystal structure of iron diselenite hydrogenselenite has been determined (6) and moreover its cell dimensions are similar to those quoted by Bertaud (3). Considering the isostructurality (Table 1), it is likely that Bertaud in fact studied the compounds $M(Se_2O_5)(HSeO_3)$, M = Fe, Cr.

The present article deals with the synthesis, the characterization, and the magnetostructural study of crystals of the title compounds.

EXPERIMENTAL

Synthesis and Characterization

Metallic oxide, M_2O_3 with M = Fe or Cr and selenium dioxide SeO_2 previously dried by sublimation (molar ratio SeO_2/M_2O_3 = 6) were introduced in outgassed sealed Pyrex tubes. The tubes were heated gradually to 673 K where they were kept for 24 h before cooling slowly. Single crystals, pale green for iron and dark green for chromium, had grown in these tubes.

Elemental analyses have been caried out for the two compounds. They were consistent with the formulation determined hereafter on single crystals, $Fe_2(Se_2O_5)_3$ abbreviated as (I) and $Cr_2(Se_2O_5)_3$ (II). For (I), calculated wt%, Fe = 13.52, Se = 57.39; observed wt%, Fe = 13.2, Se = 57.1. For (II), calculated wt%, Cr = 12.71, Se = 57.93; observed wt%, Cr = 12.5, Se = 57.9.

In both cases, X-ray powder diffraction patterns of bulk samples agreed well with those calculated from the crystal structure.

It is worth noting that the synthesis conditions must be carefully followed.

For (I), (i) traces of water enhanced the formation of $Fe(Se_2O_5)(HSeO_3)$ (6) or even of $Fe(HSeO_3)_3$ (6) and (ii) if the molar ratio SeO_2/M_2O_3 was less than six or the temperature was less than 673 K a mixture of iron diselenite and of unknown phase was observed. The latter occurred as pure phase when the value of SeO_2/M_2O_3 was three, according to its chemical analysis, thus suggesting a formula, $Fe_2(SeO_3)_3$ (calc. wt%, Fe = 22.67, Se = 48.09; obs. wt%, Fe = 23.0, Se = 47.7). Unfortunately we did not obtain single crystals of this phase.

For (II), the presence of traces of water resulted in a mixture of the phase isolated by Bertaud (3) and of the diselenite.

[1] To whom correspondence should be addressed.

0022-4596/96 $18.00

TABLE 1
Unit Cell Parameters of Some Iron(III) and Chromium(III) "Selenites"

	$Fe_2(Se_2O_5)_3$	$Cr_2(Se_2O_5)_3$	$Fe(HSeO_3)(Se_2O_5)$	$Fe(HSeO_3)_3$	$Fe_2(Se_2O_5)_3$	$Cr_2(Se_2O_5)_3$
Ref.	Bertaud (3)		Muilu *et al.* (6)		Actual work	
a (Å)	7.448(4)	7.356(5)	7.470(8)	7.460(1)	11.325(1)	10.904(1)
b (Å)	12.648(6)	12.553(8)	12.668(5)	11.597(3)	11.038(1)	11.369(2)
c (Å)	10.792(6)	10.485(8)	10.45(2)	11.360(8)	11.563(2)	11.673(2)
β (°)	134.6(2)	133.6(2)	133.82(5)	124.48(4)	102.56(1)	95.11(2)
System	Monoclinic		Monoclinic		Monoclinic	
Space group	$P2_1/c$		$P2_1/c$		$P2_1/n$	
Volume (Å^3)	723.8(2)	701.1(2)	713.9(1)	810.1(1)	1411.0(8)	1441.1(6)
Z	2		2		4	

The infrared spectra of the two new diselenites showed a complicated band structure perhaps due to the presence of three diselenite groups per asymmetric unit. Assignment of the bands, in comparison with other spectra of diselenites species (6–8), are given in Table 2. From these data it appears that the bands of (I) are more split than (II).

Crystal Structure Determination

A single crystal of both compounds was mounted on a CAD4 Enraf-Nonius diffractometer. The orientation matrix and accurate cell constants were derived from least squares refinement of the setting angles of 25 reflections. A summary of crystal data, X-ray data collection, and details of the structure refinement is listed in Table 3. The systematic absence conditions ($h0l$, $h + l = 2n$; $0k0$, $k = 2n$) led to the space group $P2_1/n$. Intensity data were corrected for absorption (ψ scans) (9). The heavy atoms, selenium and iron or chromium, were localized by the Patterson technique, the remaining oxygen atoms from successive difference Fourier maps. The final values of the atomic parameters and equivalent displacement parameters are listed in Tables 4 and 5, respectively.

TABLE 2
Infrared Absorption Frequencies in the Domain 1000–400 cm^{-1} for $Fe_2(Se_2O_5)_3$ and $Cr_2(Se_2O_5)_3$ Compounds in Comparison with $Fe(HSeO_3)(Se_2O_5)$ (10) and $MnSe_2O_5$ (4)

Assignment	$Fe_2(Se_2O_5)_3$	$Cr_2(Se_2O_5)_3$	$Fe(HSeO_3)(Se_2O_5)$	$MnSe_2O_5$
Se–O terminal	915	860	877	879
	869	775	830	858
	846	749	745	783
	781			
	749			
Se–O bridge	641	631	592	622
	606	577		
	587	533		
	548			
Se–O terminal	498	474	487	487
	463			

For (I), all the atoms were in general positions, while for (II), the chromium atoms occupied special positions (symmetry center).

Structure analysis and refinement were carried out using the program CRYSTAL (10). The last cycle including anisotropic thermal displacements and a weighting scheme converged to the final agreement factors R = 3.93 and 3.95% and Rw = 4.02 and 4.59% for (I) and (II), respectively.

The weighting scheme used was that of Tuckey and Prince (9) fitted using a Chebysev polynomial coefficient (Table 3). A final difference Fourier synthesis revealed no significant feature for both compounds.

Magnetic Measurements

Magnetic susceptibility measurements were made on powder samples of about 20 mg in the temperature range 5–300 K with a QUANTUM DESIGN SQUID susceptometer.

These powder samples were pure according to their X-ray powder diffraction patterns and their chemical analyses.

RESULTS AND DISCUSSION

Description of the Structures

Both structures crystallize in the same space group. The unit cell dimensions (Table 3) are similar; the largest discrepancy reaches 7% (β angle). The structural features of both compounds are essentially the same; three-dimensional character made by isolated octahedra of iron or chromium related by tetramonodentate diselenite groups. However, slight differences appear between the two structures.

The projection views of these two structures are shown in Figs. 1 and 2. Each iron or chromium octahedron is made by oxygen atoms belonging to six diselenite groups.

TABLE 3
Experimental Crystallographic Data for $Fe_2(Se_2O_5)_3$ and $Cr_2(Se_2O_5)_3$

Crystal data	$Fe_2(Se_2O_5)_3$	$Cr_2(Se_2O_5)_3$
Crystal system	Monoclinic	Monoclinic
Space group	$P2_1/n$	$P2_1/n$
a (Å)	11.325(1)	10.904(1)
b (Å)	11.038(1)	11.369(2)
c (Å)	11.563(2)	11.673(2)
β (°)	102.56(1)	95.11(2)
V (Å^3)	1411.0(8)	1441.1(6)
Z	4	4
Molecular weight (g)	825.44	817.74
ρ calc. (g · cm^{-3})	3.886	3.769
μ (Mo$K\alpha$)(cm^{-1})	174.63	165.55
Crystal size (mm)	0.1 × 0.2 × 0.15	0.2 × 0.2 × 0.07
Transmission coef. range	0.53–1.00	0.32–1.00
Data collection		
Temperature (K)	293	293
Wavelength (Mo$K\alpha$) (Å)	0.71073	0.71073
Monochromator	Graphite	Graphite
Scan mode	$\Omega - 2\theta$	$\Omega - 2\theta$
Scan width (°)	0.80 + 0.35 tan θ	0.80 + 0.35 tan θ
Take-off angle (θ)	2.3	3
Max Bragg angle	25	28
hkl	$0 \rightarrow 13$, $0 \rightarrow 13$, $-13 \rightarrow 13$	$0 \rightarrow 14$, $0 \rightarrow 15$, $-15 \rightarrow 15$
Structure refinement		
Reflections collected	2857	3833
Unique reflections used ($I > 3\sigma(I)$)	1620	2046
Number of refined parameters	134	140
$R = \Sigma\|\|Fo\| - \|Fc\|\|/\Sigma\|Fo\|$	0.039	0.039
$Rw = [\Sigma w(\|Fo\| - \|Fc\|)^2/\Sigma wFo^2]^{1/2}$	0.040	0.046
weighting with 3 coefficients (see text)	1.98 −1.18 0.80	3.63 −1.43 2.33

The three crystallographically distinct diselenite groups bridge four metallic atoms (two times Fe1 and two times Fe2 or Cr1, Cr2, Cr3, and Cr4). Two diselenite groups namely Se3–Se4, Se5–Se6, and the metal atoms build sheets along the (001) plane (Fig. 1 and 2). These sheets are interconnected by the third diselenite group, Se1–Se2 (Fig. 3 and 4). It is worthwhile to notice the analogy of these latter figures showing up the linkage of the sheets (Fig. 1 and 2) by the third diselenite group Se1–Se2. The smallest intermetallic distances are not very different, 5.5404(6) Å for (I) and 5.4507(5) Å for (II) (Tables 6, 7).

Iron octahedra are more distorted than chromium ones. Fe–O distances range from 1.94(1) to 2.039(9) Å (Table 6). The mean Fe–O bonds for Fe1 and Fe2 amount to 1.99 Å which agrees quite well with the mean value of 2.01 known for ferric iron (6, 11–17). The O–Fe–O angles either for Fe1 or Fe2 differ from 90° or 180° by almost 10° (Table 6).

Mean bond lengths within the chromium polyhedra are comparable with average distances ranging from 1.965 to 1.970 Å (Table 7). The variations of O–Cr–O angles from 90° do not exceed 4.1°.

The geometry of the diselenite groups in both structures is practically comparable to that of several other diselenite compounds ($ZnSe_2O_5$ (18), $CoSe_2O_5$ (19), $CuSe_2O_5$ (20), $VOSe_2O_5$ (21), $MnSe_2O_5$ (7, 8), $LiFe(Se_2O_5)$ (16), and $PbSe_2O_5$ (22)).

The distances Se–O of the Se–O–Se bridge are marginally longer than the terminal Se–O bonds (Tables 6, 7). For (II), one angle Se3–O6–Se4, 116.7(6), differs slightly from the others, but this value is included in the angles range currently observed (117.1(5)° for $PbSe_2O_5$ (22) to 136.9(2)° in monoclinic $MnSe_2O_5$ (7)). Although the geometry of the diselenite group is practically unchanged, its coordination mode can vary: (i) bischelation for $CuSe_2O_5$ (20); (ii) chelation and two times monodentate in $MnSe_2O_5$ (7, 8) or compounds listed in (16, 18, 19); (iii) tetramonodentate in $VOSe_2O_5$ (21), (I) and (II) diselenite.

Thermal Behavior

Thermal analyses of both compounds were realized on a Setaram TG 85 apparatus, using 20 mg, in a flow of $He–O_2$ (1/1) at a heating rate of 5 K/min. They are presented in Fig. 5.

TABLE 4
Positional Atomic Parameters and Thermal Equivalent Parameters for $Fe_2(Se_2O_5)_3$

Atom	x	y	z	B_{eq}[a](Å^2)
Fe1	0.7411(1)	0.7413(1)	0.2263(1)	0.96(6)
Fe2	0.2595(2)	0.2390(2)	0.2709(1)	1.30(7)
Se1	0.2477(1)	0.4054(1)	0.5092(1)	2.64(6)
Se2	0.3629(1)	0.6624(1)	0.5077(1)	1.52(5)
Se3	0.4854(1)	0.5950(2)	0.2098(1)	1.18(5)
Se4	0.4789(1)	0.3259(1)	0.1220(1)	1.37(5)
Se5	−0.1731(1)	0.4806(1)	0.1545(1)	1.11(4)
Se6	0.1041(1)	0.4847(1)	0.2074(1)	1.42(5)
O1	0.3663(7)	0.5124(8)	0.5674(7)	1.9(1)[b]
O2	0.3063(9)	0.3556(9)	0.3983(8)	2.6(2)[b]
O3	0.294(1)	0.300(1)	0.6128(9)	3.4(2)[b]
O4	0.2928(8)	0.6256(8)	0.369(1)	2.1(2)[b]
O5	0.2492(9)	0.7213(9)	0.5605(9)	3.0(2)[b]
O6	0.4258(7)	0.4792(8)	0.1010(7)	1.7(1)[b]
O7	0.3861(7)	0.7017(8)	0.1579(7)	1.7(1)[b]
O8	0.6033(7)	0.6371(8)	0.1503(7)	1.6(1)[b]
O9	0.4143(9)	0.2796(9)	0.2292(8)	2.7(2)[b]
O10	0.6210(8)	0.3508(8)	0.1981(7)	1.9(2)[b]
O11	−0.037(1)	0.478(1)	0.1049(9)	3.5(2)[b]
O12	−0.140(1)	0.382(1)	0.266(1)	3.6(2)[b]
O13	−0.146(1)	0.605(1)	0.239(1)	4.8(3)[b]
O14	0.1641(8)	0.3614(8)	0.1593(8)	2.0(2)[b]
O15	0.1626(7)	0.5962(8)	0.1411(7)	1.6(1)[b]

[a] $B_{eq} = 8\pi^2/3\Sigma_i\Sigma_j U(i,j)a_i^*a_j^*a_ia_j$, a^* reciprocal parameter.
[b] Atoms refined isotropically.

The weight losses are compatible with the following equations:

$$Fe_2(Se_2O_5)_3 \xrightarrow[\Delta m1]{} Fe_2(SeO_3)_3 + 3SeO_2 \qquad T = 673\text{–}733\ K$$

$$Fe_2(SeO_3)_3 \xrightarrow[\Delta m2]{} Fe_2O_3 + 3SeO_2 \qquad T = 793\text{–}843\ K$$

$$Cr_2(Se_2O_3)_3 \xrightarrow[\Delta m]{} Cr_2O_3 + 6SeO_2 \qquad T = 723\text{–}783\ K.$$

The curve for (I) presents a double step process starting at 663 K, with an intermediate phase between 733 and 793 K; constant weight (Fe_2O_3) is achieved at 843 K. The weight loss observed for the intermediate phase is in accordance with the presence of $Fe_2(SeO_3)_3$. Two endothermic peaks around 683 and 803 K mark this decomposition.

Muilu *et al.* studied the decomposition of $Fe(Se_2O_5)(HSeO_3)$, and no intermediate phase was observed (6). These authors claim that this stability is due to the structure itself. The thermal analysis of $Fe_2(SeO_3)_3 \cdot 6H_2O$ gave an intermediate oxyselenite (23), which is not observed here.

For (II), no intemediate phase is observed and six SeO_2 molecules per formula unit are lost, leading to Cr_2O_3, occuring in the temperature range between 723 and 793 K. One broad endothermic peak around 773 K marks this decomposition. The thermal behavior of $Cr_2(Se_2O_5)_2$ is rather strange; usually except for the $Fe(Se_2O_5)(HSeO_3)$ compound the thermal decomposition of the diselenite gives the monoselenite.

When it is exposed to water pressure at room temperature (pH_2O = 20 Torr) the diselenites of iron or chromium are unstable. The well crystallized phases $Fe(Se_2O_5)(HSeO_3)$ and $Fe(HSeO_3)_3$ are observed after 1 or 3 years, respectively.

For the chromium diselenite, its evolution kinetics is slower: after 3 years the $Cr(Se_2O_5)(HSeO_3)$ phase is present.

Magnetic Measurements

Magnetic susceptibilities per mole of either Fe or Cr are presented in Figs. 6 and 7, respectively, as χ_M and $\chi_{M^{-1}} = f(T)$ in the temperature range 300–5 K.

In the high-temperature limit (300–50 K), both compounds follow a Curie–Weiss law, i.e., $\chi_M = C/(T - \theta)$. The curie constants C = 4.73 cm^{3}mol^{-1}K for (I) and C = 1.72 cm^{3}mol^{-1}K for (II) are compatible with high spin S = 5/2 and S = 3/2, respectively. The negative Weiss constants θ = −65 K for (I) and θ = −10 K for (II) are

TABLE 5
Positional Atomic Parameters and Thermal Equivalent Parameters for $Cr_2(Se_2O_5)_3$

Atom	x	y	z	B_{eq}[a](Å^2)
Cr1	1/2	1/2	0	0.65(7)
Cr2	0	1/2	0	0.63(7)
Cr3	1/2	0	0	0.63(7)
Cr4	0	0	0	0.67(7)
Se1	0.36053(9)	0.53372(9)	0.24172(8)	1.03(4)
Se2	0.08903(8)	0.45256(9)	0.25350(8)	0.89(3)
Se3	0.76630(8)	0.10718(8)	0.10984(8)	0.88(3)
Se4	0.75105(8)	0.36876(8)	0.04983(8)	0.77(3)
Se5	0.37102(9)	0.24778(8)	−0.01527(8)	0.92(3)
Se6	0.08856(8)	0.24631(9)	−0.08125(8)	0.92(3)
O1	0.2501(7)	0.4285(7)	0.2837(7)	1.8(1)[b]
O2	0.3817(6)	0.4706(6)	0.1150(6)	1.1(1)[b]
O3	0.4781(6)	0.4835(6)	0.3292(6)	1.2(1)[b]
O4	0.0619(7)	0.5495(7)	0.3542(6)	1.5(1)[b]
O5	0.0960(6)	0.5467(6)	0.1419(6)	1.0(1)[b]
O6	0.7757(6)	0.2551(6)	0.1585(6)	1.1(1)[b]
O7	0.8716(6)	0.1171(6)	0.0137(6)	1.1(1)[b]
O8	0.6339(7)	0.1175(6)	0.0243(6)	1.3(1)[b]
O9	0.8675(6)	0.4575(6)	0.0973(6)	1.0(1)[b]
O10	0.6319(6)	0.4317(6)	0.1054(6)	1.1(1)[b]
O11	0.2388(7)	0.2893(7)	−0.1098(6)	1.4(1)[b]
O12	0.4021(6)	0.1218(6)	−0.0829(6)	0.9(1)[b]
O13	0.4666(6)	0.3442(6)	−0.0704(6)	1.1(1)[b]
O14	0.0633(6)	0.3390(6)	0.0248(6)	1.2(1)[b]
O15	0.1258(6)	0.1237(6)	−0.0043(6)	1.1(1)[b]

[a] $B_{eq} = 8\pi^2/3\Sigma_i\Sigma_j U(i,j)a_i^*a_j^*a_ia_j$, a^* reciprocal parameter.
[b] Atoms refined isotropically.

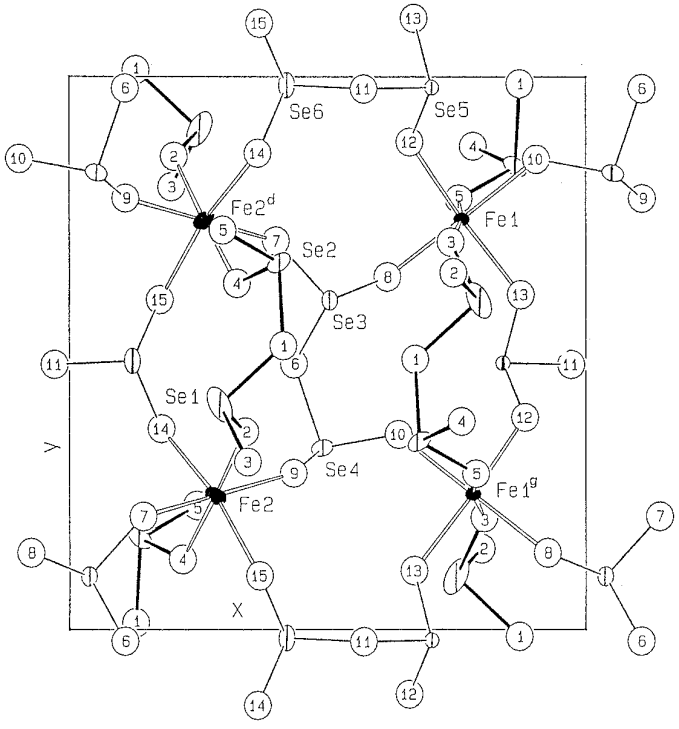

FIG. 1. Projection of $Fe_2(Se_2O_5)_3$ along the vector [001] of a single sheet showing the atom labeling scheme.

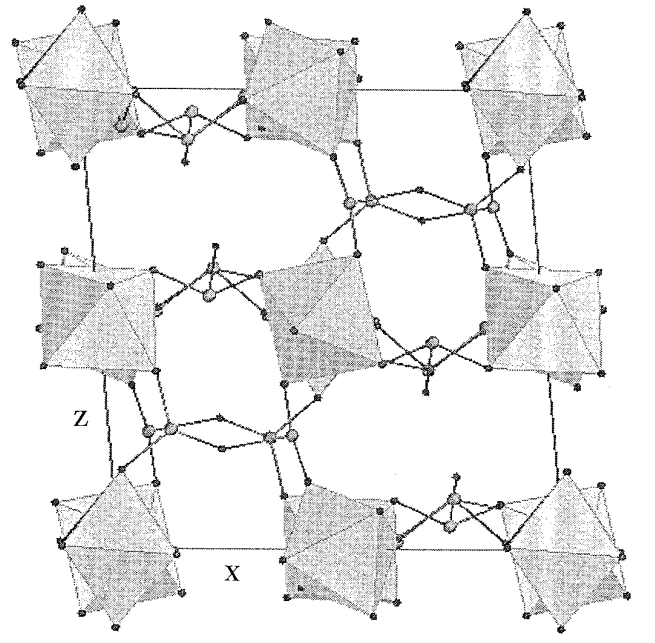

FIG. 3. View of $Fe_2(Se_2O_5)_3$ along the vector [100] illustrating the bonding of the sheet by Se1–Se2 diselenite group.

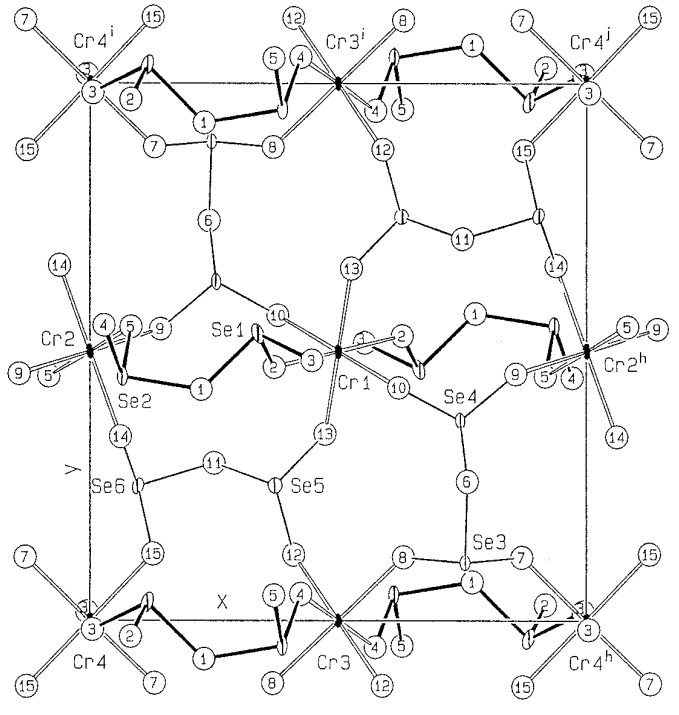

FIG. 2. Projection of $Cr_2(Se_2O_5)_3$ along the vector [001] of a single sheet showing the atom labeling scheme.

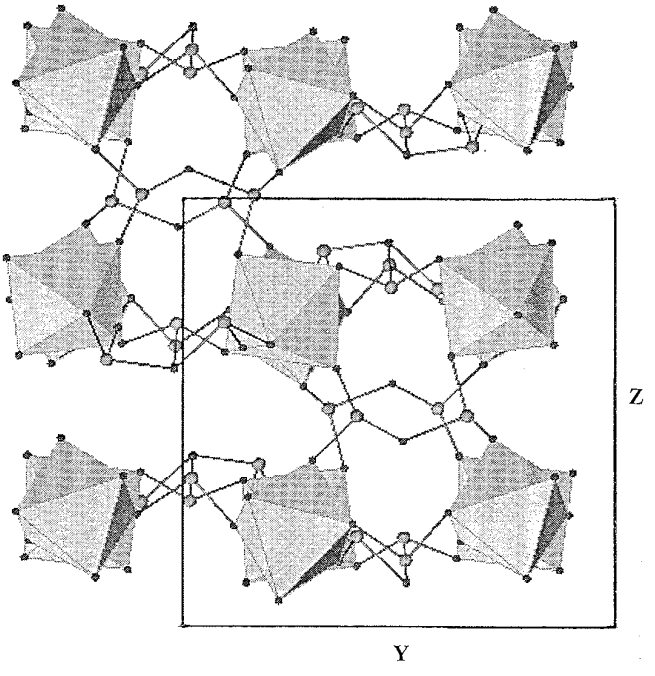

FIG. 4. View of $Cr_2(Se_2O_5)_3$ along the vector [010] illustrating the bonding of the sheet by Se1–Se2 diselenite group.

TABLE 6
Selected Interatomic Distances (Å) and Angles (°) for $Fe_2(Se_2O_5)_3$

	Fe1 environment		
Fe1–O3[a]	2.04(1)	O5[b]–Fe1–O3[a]	171.5(4)
Fe1–O5[b]	1.98(1)	O8–Fe1–O3[a]	89.1(4)
Fe1–O8	1.984(8)	O5[b]–Fe1–O8	83.6(4)
Fe1–O10[c]	2.018(8)	O10[c]–Fe1–O3[a]	91.4(4)
Fe1–O12[d]	1.95(1)	O12[d]–Fe1–O3[a]	84.4(4)
Fe1–O13[e]	1.96(1)	O13[e]–Fe1–O3[a]	90.8(5)
		O5[b]–Fe1–O10[c]	95.7(4)
⟨Fe1–O⟩	1.985	O12[d]–Fe1–O5[b]	91.7(4)
		O13[e]–Fe1–O5[a]	93.7(5)
		O8–Fe1–O10[c]	178.6(3)
		O12[d]–Fe1–O8	93.8(4)
		O13[e]–Fe1–O8	91.6(4)
		O12[d]–Fe1–O10[c]	84.9(4)
		O13[e]–Fe1–O10[c]	89.7(5)
		O12[d]–Fe1–O13[e]	172.7(4)
	Fe2 environment		
Fe2–O2	1.940(9)	O2–Fe2–O4[f]	176.6(4)
Fe2–O4[f]	2.03(1)	O2–Fe2–O7[f]	86.4(4)
Fe2–O7[f]	2.039(9)	O2–Fe2–O9	85.6(4)
Fe2–O9	1.96(7)	O2–Fe2–O14	93.5(4)
Fe2–O14	2.013(8)	O2–Fe2–O15[f]	96.9(4)
Fe2–O15[f]	1.977(8)	O4[f]–Fe2–O7[f]	94.2(4)
		O9–Fe2–O4[f]	93.9(4)
⟨Fe2–O⟩	1.993	O9–Fe2–O7[f]	170.6(3)
		O9–Fe2–O14	94.1(4)
		O9–Fe2–O15[f]	89.2(4)
		O14–Fe2–O4[f]	83.1(4)
		O14–Fe2–O7[f]	91.4(4)
		O15[f]–Fe2–O4[f]	86.4(3)
		O15[f]–Fe2–O7[f]	86.6(3)
		O15[f]–Fe2–O14	169.2(3)
Fe2–Fe2[d]	5.5404(6)		
Fe2–Fe2[f]	5.540(6)		
Fe2–Fe1[g]	5.648(2)		
Fe2–Fe1[f]	5.677(2)		
Fe2–Fe1[a]	5.819(2)		
Fe2–Fe1[h]	5.752(2)		

TABLE 6—*Continued*

	Se environment		
Se1–O1	1.805(8)	O2–Se1–O3	102.1(5)
Se1–O2	1.65(1)	O2–Se1–O1	96.6(4)
Se1–O3	1.66(1)	O3–Se1–O1	95.5(4)
Se2–O1	1.791(8)	O4–Se2–O5	101.6(4)
Se2–O4	1.68(1)	O4–Se2–O1	96.3(4)
Se2–O5	1.67(1)	O5–Se2–O1	99.9(4)
Se3–O6	1.820(8)	Se1–O1–Se2	120.6(4)
Se3–O7	1.655(8)	O7–Se3–O8	101.1(4)
Se3–O8	1.684(9)	O7–Se3–O6	97.0(4)
Se4–O6	1.794(8)	O8–Se3–O6	97.0(4)
Se4–O9	1.65(1)	O9–Se4–O10	100.8(4)
Se4–O10	1.680(1)	O9–Se4–O6	101.7(4)
Se5–O11	1.75(1)	O10–Se4–O6	99.8(4)
Se5–O12	1.66(1)	Se3–O6–Se4	120.2(4)
Se5–O13	1.67(1)	O12–Se5–O13	95.9(6)
Se6–O11	1.773(9)	O12–Se5–O11	99.9(5)
Se6–O14	1.670(9)	O13–Se5–O11	97.8(6)
Se6–O15	1.662(8)	O14–Se6–O15	102.5(4)
		O14–Se6–O11	96.5(4)
		O15–Se6–O11	96.7(4)
		Se5–O11–Se6	120.5(6)

[a] $1 - x, 1 - y, 1 - z$.
[b] $1/2 + x, 3/2 - y, z - 1/2$.
[c] $3/2 + x, 1/2 + y, 1/2 - z$.
[d] $1/2 - x, 1/2 + y, 1/2 - z$.
[e] $1 + x, y, z$.
[f] $1/2 - x, y - 1/2, 1/2 - z$.
[g] $3/2 - x, y - 1/2, 1/2 - z$.
[h] $1 - x, 1 - y, -z$.

indicative of weak antiferromagnetic coupling between the iron or chromium atoms.

Tentatives have been made to extract the exchange interaction between metallic atoms. Since iron(III) and chromium(III) have nondegenerate orbital ground state ($^6A_1$ and $^4A_2$), the exchange interaction is expected to be properly described by an isotropic Heisenberg Hamiltonian (24). There is no closed-form theory available for the three-dimensional system, only limited expansions of the susceptibility are known. As long as the number of nearest magnetic neighbors for Fe^{3+} or Cr^{3+} is six,[2] one can reasonably use the high-temperature series expansion given by Lines (25) on ''simple cubic lattice'' which is the closest available model. In that framework, if the nearest-neighbor interaction is written as JS_iS_j, (where positive J is indicative of antiferromagnetic interaction and S_i is a spin operator at the site i) one can write

$$\chi = \frac{N\beta^2}{3kT} g^2 S(S+1)\left[1 - \sum_{i=1}^{10} Bi/\theta^i\right],$$

in which $\theta = kT/JS(S+1)$ and $B1 = 2.0000$, $B2 = -3.3333$, $B3 = 5.3333$, $B4 = -8.2222$, $B5 = 12.4444$, $B6 = -18.4856$, $B7 = 27.1276$, $B8 = -39.3772$, $B9 = 56.6914$, and $B10 = -81.0260$. Such an expression only holds in the high-temperature range and it is important to know how far the limited expansion is valid at low temperature. To answer this question, several fittings have been made by varying the temperature range; using g and J/k as adjustable parameters,

—for (I), over the temperature range 300–60 K, a good agreement is obtained with $J/k = 2.9$ K and $g = 2.02$ ($R = 0.15 \times 10^{-3}$)(26), and

—for (II), over the temperature range 300–130 K, an excellent agreement is obtained with $J/k = 4.5$ K and $g = 2.01$ ($R = 0.91 \times 10^{-4}$).

Calculated curves using these parameters are shown on

[2] For $Fe_2(Se_2O_5)_3$ the iron–iron distance goes from 5.5404(6) to 5.819(2) Å and for $Cr_2(Se_2O_5)_3$ the chromium–chromium distance is from 5.4507(5) to 5.836(1) Å.

TABLE 7
Selected Interatomic Distances (Å) and Angles (°) for $Cr_2(Se_2O_5)_3$

		Cr1 environment	
Cr1–O2	1.970(7)	O10–Cr1–O2	89.6(2)
Cr1–O10	1.968(6)	O10–Cr1–O2[a]	90.4(3)
Cr1–O13	1.973(6)	O10–Cr1–O13[a]	89.8(2)
		O10–Cr1–O13	90.2(2)
⟨Cr1–O⟩	1.970	O2[a]–Cr1–O13	91.3(3)
		O2[a]–Cr1–O13[a]	88.6(4)
		Cr2 environment	
Cr2–O5	1.952(6)	O5–Cr2–O9[a]	93.2(3)
Cr2–O9[b]	1.974(7)	O5–Cr2–O9[b]	86.7(3)
Cr2–O14	1.968(7)	O5–Cr2–O14	88.5(3)
		O5–Cr2–O14[c]	91.5(3)
⟨Cr2–O⟩	1.965	O14–Cr2–O9[a]	92.7(3)
		O14–Cr2–O9[b]	87.3(3)
		Cr3 environment	
Cr3–O4[d]	1.967(7)	O4[d]–Cr3–O8	89.3(3)
Cr3–O8	1.980(7)	O4[d]–Cr3–O8[f]	90.7(3)
Cr3–O12	1.952(6)	O12–Cr3–O4[d]	90.6(3)
		O12–Cr3–O4[e]	89.4(3)
⟨Cr3–O⟩	1.966	O12–Cr3–O8	87.5(3)
		O12–Cr3–O8[f]	92.5(3)
		Cr4 environment	
Cr4–O3[d]	1.996(7)	O15–Cr4–O3[d]	94.1(3)
Cr4–O7[b]	1.948(7)	O15–Cr4–O3[e]	85.9(3)
Cr4–O15	1.967(7)	O7[b]–Cr4–O3[d]	90.3(3)
		O7[b]–Cr4–O3[e]	89.7(3)
⟨Cr4–O⟩	1.970	O7[f]–Cr4–O15	88.8(3)
		O7[f]–Cr4–O15[g]	91.2(3)
Cr1–Cr2	5.4507(5)		
Cr1–Cr3	5.684(1)		
Cr1–Cr4	5.836(1)		

TABLE 7—*Continued*

		Se environment	
Se1–O1	1.795(8)	O2–Se1–O1	95.9(3)
Se1–O2	1.678(7)	O3–Se1–O1	95.8(3)
Se1–O3	1.666(7)	O3–Se1–O2	103.6(3)
Se2–O1	1.781(1)	O5–Se2–O1	97.9(3)
Se2–O4	1.657(7)	O4–Se2–O1	101.3(3)
Se2–O5	1.693(6)	O4–Se2–O5	98.5(3)
Se3–O6	1.775(7)	Se1–O1–Se2	121.0(4)
Se3–O7	1.678(7)	O8–Se3–O6	98.4(3)
Se3–O8	1.685(7)	O7–Se3–O6	97.3(3)
Se4–O6	1.814(7)	O7–Se3–O8	101.5(3)
Se4–O9	1.676(6)	O9–Se4–O6	97.8(3)
Se4–O10	1.663(7)	O10–Se4–O6	96.0(3)
Se5–O11	1.799(7)	O10–Se4–O9	101.9(3)
Se5–O12	1.684(6)	Se3–O6–Se4	116.7(6)
Se5–O13	1.679(7)	O12–Se5–O11	96.8(3)
Se6–O11	1.768(7)	O13–Se5–O11	94.8(3)
Se6–O14	1.666(7)	O13–Se5–O12	102.6(3)
Se6–O15	1.688(7)	O15–Se6–O11	98.4(3)
		O14–Se6–O11	100.4(3)
		O14–Se6–O15	100.0(3)
		Se5–O11–Se6	121.1(4)

[a] $1 - x, 1 - y, -z$.
[b] $x - 1, y, z$.
[c] $-x, 1 - y, -z$.
[d] $1/2 - x, y - 1/2, 1/2 - z$.
[e] $1/2 + x, 1/2 - y, z - 1/2$.
[f] $1 - x, -y, -z$.
[g] $-x, -y, -z$.

Figs. 6 and 7. It has to be noted that if the lower temperature is dropped, the agreement is still good but the g parameter deviates from the expected value $g = 2.00$ which is the one commonly accepted for Fe^{3+} and Cr^{3+}. (As an example; for (II), over the temperature range 300–10 K, the result of the fitting gave $J/k = 0.65$ K, $g = 1.82$, and $R = 0.2610^{-3}$. Although the agreement is good, the result does not seem realistic.)

Therefore, $Fe_2(Se_2O_5)_3$ and $Cr_2(Se_2O_5)_3$ behave as a three-dimensional isotropic antiferromagnet at least down to 60 or 130 K, respectively.

At low temperature (I) presents a net increase of the inverse molar susceptibility at $T = 32$ K which is probably due to a transition to a long-range antiferromagnetic ordering. This behavior has already been observed in manganese diselenites compounds (7). However the structure of this last compound presents zigzagging chains of octahedra $[MnO_6]$ interconnected by $Se_2O_5^{2-}$ anions instead of the three-dimensional network observed for (I) and also for (II). This last feature may explain why the critical tempera-

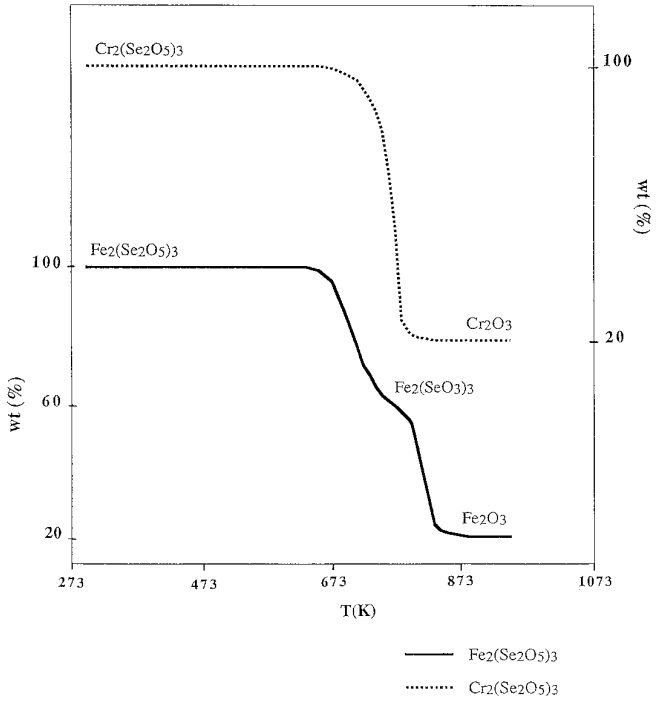

FIG. 5. Thermal gravimetry curves of $Fe_2(Se_2O_5)_3$ and of $Cr_2(Se_2O_5)_3$.

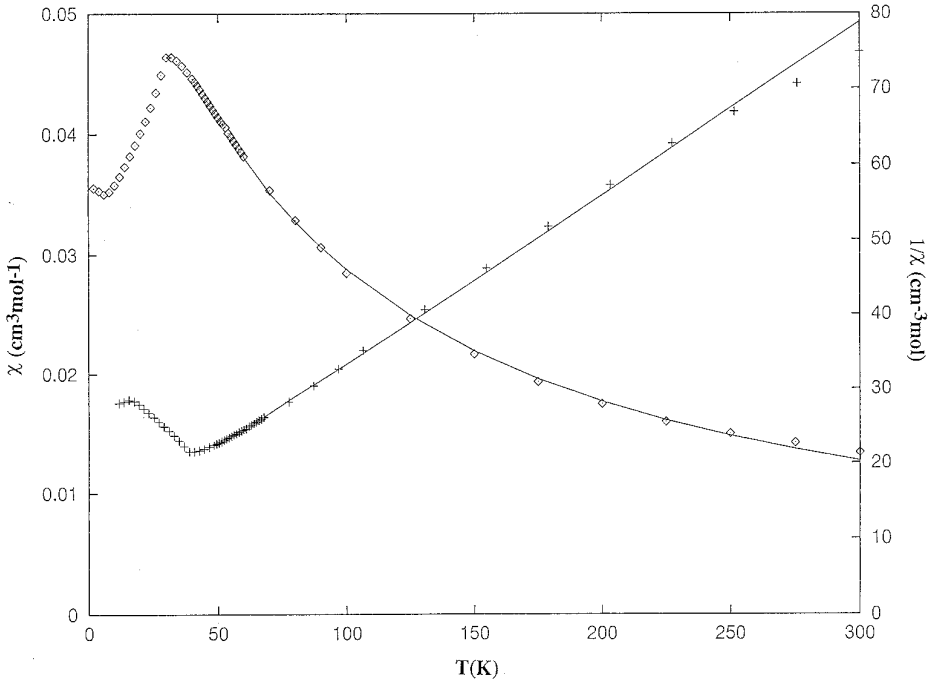

FIG. 6. Molar (⊡) and inverse molar (×) susceptibility (per mole of iron) vs temperature from 300–5 K. The solid lines are calculated using expression 1 (cf. text) in the temperature range 300–60 K with $J/k = 2.9$ K, $g = 2.02$, and $R = 0.15 \times 10^{-3}$.

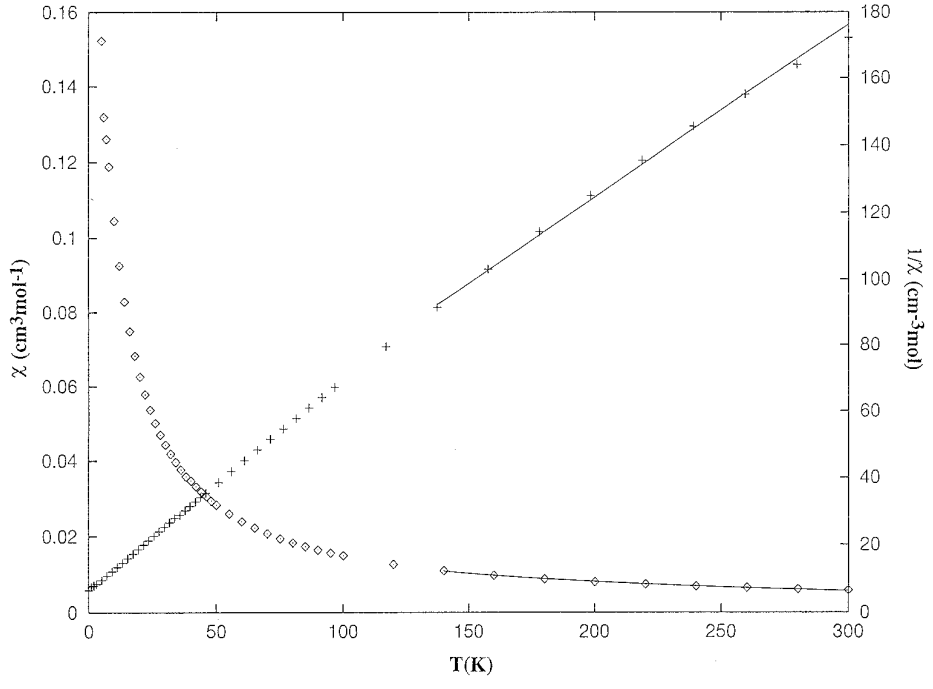

FIG. 7. Molar (⊡) and inverse molar (×) susceptibility (per mole of chromium) vs temperature from 300–5 K. The solid lines are calculated using expression 1 (cf. text) in the temperature range 300–130 K with $J/k = 4.5$ K, $g = 2.01$, and $R = 0.91 \times 10^{-4}$.

ture is higher ($T = 32$ K) than the one observed for the manganese diselenite compounds ($T = 9$ K) (7).

Open questions remain on the different magnetic behavior at low temperature for (I) and (II). Even though (I) and (II) have a practically similar structure, (II) does not present any long-range antiferromagnetic ordering.

See NAPS document No. 05289 for 24 pages of supplementary material. Order from ASIS/NAPS. Microfiche Publications, P.O. Box 3513, Grand Central Station, New York, NY 10163. Remit in advance $4.00 for microfiche copy or for photocopy, $7.75 up to 20 pages plus $.30 for each additional page. All orders must be prepaid. Institutions and Organizations may order by purchase order. However, there is billing and handling charge for this service of $15. Foreign orders add $4.50 for postage and handling, for the first 20 pages, and $1.00 for additional 10 pages of material, $1.50 for postage of any microfiche orders.

REFERENCES

1. O. Kahn, M. Verdaguer, J. J. Girerd, J. Galy, and F. Maury, *Solid State Commun.* **34,** 971 (1980).
2. J. C. Trombe, A. Gleizes, J. Galy, J. P. Renard, Y. Journaux, and M. Verdaguer, *New J. Chem.* **11,** 321 (1987).
3. M. Bertaud, Thesis, Bordeaux, France, 1974.
4. A. M. Lafront and J. C. Trombe, *Inorg. Chim. Acta* **234,** 19 (1995).
5. A. M. Lafront, J. C. Trombe, and J. Bonvoisin, *Inorg. Chim. Acta* **238,** 15 (1995).
6. H. Muilu and J. Valkonen, *Acta Chem. Scand. Ser. A* **41,** 183 (1987).
7. J. Bonvoisin, J. Galy, and J. C. Trombe, *J. Solid State Chem.* **107,** 171 (1993).
8. M. Koskenlinna, L. Niinisto, and J. Valkonen, *Cryst. Struct. Commun.* **5,** 663 (1976); *Acta Chem. Scand. Ser. A* **30,** 836 (1976).
9. J. R. Carruthers and D. J. Watkin, *Acta Crystallogr. Sect. A* **35,** 698 (1979).
10. J. D. Watkin, J. R. Carruthers, and P. W. Bette Ridge, "Crystal User's Guide." Chemical Crystallography Laboratory, Univ. of Oxford, Oxford, 1986.
11. J. Valkonen and M. Koskenlinna, *Acta Chem. Scand. Ser. A* **32,** 603 (1978).
12. F. C. Hawthorne, *Can. Miner.* **22,** 475 (1984).
13. G. Giester, *Mh. Chem.* **123,** 957 (1992).
14. G. Giester, *J. Solid State Chem.* **103,** 451 (1993).
15. G. Giester, *Z. Kristallogr.* **207,** 1 (1993).
16. G. Giester, *Mh. Chem.* **124,** 1107 (1993).
17. G. Giester and F. Pertlik, *J. Alloys Compounds* **210,** 125 (1994).
18. G. Meunier and M. Bertaud, *Acta Crystallogr. Sect. B* **30,** 2840 (1974).
19. F. C. Hawthorne, L. A. Groat, and T. S. Ercit, *Acta Crystallogr. Sect. C* **43,** 2042 (1987).
20. G. Meunier, C. Svensson, and A. Carpy, *Acta Crystallogr. Sect. B* **32,** 2664 (1976).
21. G. Meunier, M. Bertaud, and J. Galy, *Acta Crystallogr. Sect. B* **30,** 2834 (1974).
22. M. Koskenlinna, *Acta Crystallogr. Sect. C* **51,** 1 (1995).
23. D. Rai, S. V. Mattigod, and D. A. Moore, *Mater. Res. Bull.* **23,** 152 (1988).
24. R. L. Carlin, "Magnetochemistry" Chap. 6. Springer-Verlag, Berlin/New York, 1986.
25. M. E. Lines, *J. Phys. Chem. Solids* **31,** 101 (1970).
26. $R = \Sigma (\chi \exp - \chi \mathrm{calc})^2 / \Sigma (\chi \exp)^2$